Oil & Natural Gas Technology

DOE Award No.: DE-FE0009897

Quarterly Research Performance Progress Report (Period ending 12/31/2013)

Hydrate-Bearing Clayey Sediments: Morphology, Physical Properties, Production and Engineering/Geological Implications

Project Period (10/1/2012 to 9/30/2016)

Submitted by:
J. Carlos Santamarina

Georgia Institute of Technology
DUNS #: 097394084
505 10th street
Atlanta , GA 30332
e-mail: jcs@gatech.edu
Phone number: (404) 894-7605

Prepared for:
United States Department of Energy
National Energy Technology Laboratory

Submission date: 01/31/2014

Office of Fossil Energy

DISCLAIMER:

ACCOMPLISHMENTS

Context – Goals. *Fine grained sediments host more than 90% of the global gas hydrate accumulations. Yet, hydrate formation in clayey sediments is least understood and characterized. This research focuses on* <u>*hydrate bearing clayey sediments*</u>*. The goals of this research are (1) to gain a fundamental understanding of hydrate formation and ensuing morphology, (2) to develop laboratory techniques to emulate "natural" formations, (3) to assess and develop analytical tools to predict physical properties, (4) to evaluate engineering and geological implications, and (5) to advance gas production alternatives to recover methane from these sediments.*

Accomplished

The main accomplishments for this period include:

- X-ray CT system calibration
    - Attainable image resolution
    - Design of specimen centering positioner for rotary stage
- Design and Fabrication of new high pressure chamber
    - Light, thin-walled design for X-ray CT scanning
- Analysis of effective thermal conductivity
    - Numerical solutions
- In-Lab CO_2 hydrate formation in diatoms
- In-Lab THF hydrate formation in various sediments
    - Hydrate formation in diatoms, kaolinite, and silica flour

Plan - Next reporting period

Advance numerical and analytical solutions of physical properties of hydrate-bearing clayey sediments, including stiffness and strength. Conduct new methods of forming gas hydrate in fine-grained sediments. Design and construct cooling system for hydrate formation inside of X-ray scanning cabinet. Begin conducting measurements of physical properties of hydrate-bearing fine-grained sediments.

Research in Progress

X-ray CT Calibration

An attachment was designed and fabricated for the motorized rotary stage to attain higher accuracy in centering and positioning specimens. The result is higher quality reconstructed images due to reduced motion blurring and off-center reconstruction artifacts.

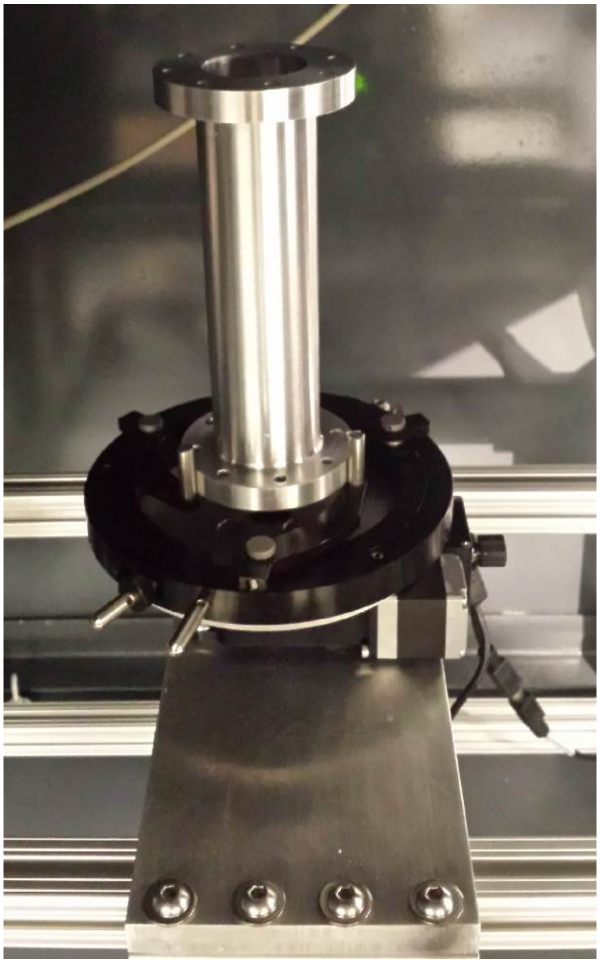

Figure 1. Motorized rotary stage with centering device.

Additionally, the system was tested to determine the minimal particle size capable of being detected at varying chamber sizes and geometric magnification distances.

Chamber Design

A thin-walled (3.5 mm) aluminum chamber (Ø 40mm, H 140mm) was designed and fabricated to sustain pressures up to 20 MPa. The end caps are made of steel with a total of 6 NPT ports for fluid and electronics feed through.

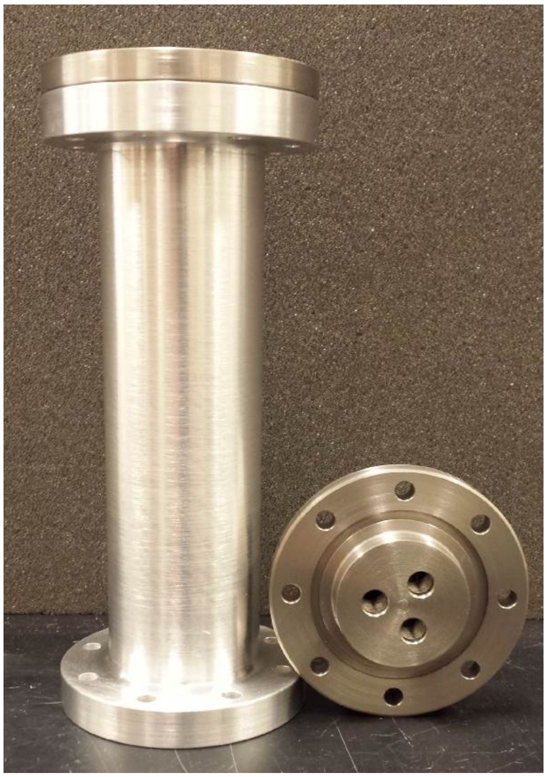

Figure 2. Thin-walled aluminum high pressure chamber and steel end caps

Effective Thermal Conductivity

A series of numerical models were implemented to narrow the range of effective thermal conductivities of hydrate-bearing fine-grained sediments with segregated hydrate morphology. The thermal properties of the segregated components were used for input into the numerical models (Table 1).

Table 1. Thermal Properties of relative components in a Hydrate-Bearing Sediment system

	λ [W m^{-1} K^{-1}]	**κ [x10^{-7} m^2 s^{-1}]**	**c_p [J kg^{-1} K^{-1}]**	**ρ [kg m^{-3}]**
Air	0.024[d]	183[d]	1010[d]	1.3[d]
Water	0.56[d]	1.33[d]	4220[d]	999.9[d]
Ice	2.18[d]	11.7[d]	2052[d]	917[d]
THF·17H_2O	0.47[a]	3.12	4080	982
THF·17H_2O hydrate	0.51[c]	2.55[e]	2020[e]	971[e]
CH_4·6H_2O hydrate	0.575[c]	3.35[f]	2031[f]	979[f]
Dry clay	0.17[a]	1.59	1700	1600
Saturated marine clay	1.12[b]	3.36[b]	1960[b]	1760[b]

References: a) Cortes et al. 2009, b) Expedition 301 Scientists 2005, c) Huang and Fan 2005, d) Kaye and Laby 2007, e) Waite et al. 2006, f) Waite et al. 2007

The validity of numerical results were compared against known analytical solution for simple cases. The model involved 3 thick layers of saturated marine clay and 2 thin hydrate layers in series.

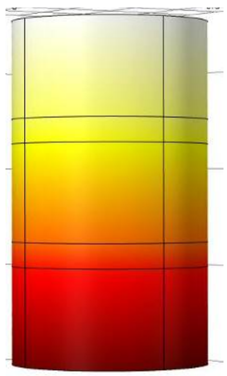

$$k_{eff,z} = L_T \left(\frac{k_{hyd} \cdot k_{clay}}{2L_{hdy} \cdot k_{clay} + 3L_{clay} \cdot k_{hyd}} \right)$$

Solution Method	**$k_{eff,z}$ [W m^{-1} K^{-1}]**
COMSOL	0.9514579
Analytical	0.9514563

Figure 3. Verification Model – Saturated marine clay + THF hydrate in series

The following study involved real hydrate structures extracted from X-ray images (a laboratory formed THF hydrate in kaolinite obtained in our lab, and in-situ natural gas hydrate in a fine-grained marine sediment from the Krishna-Godavari Basin - Priest et al. 2008).

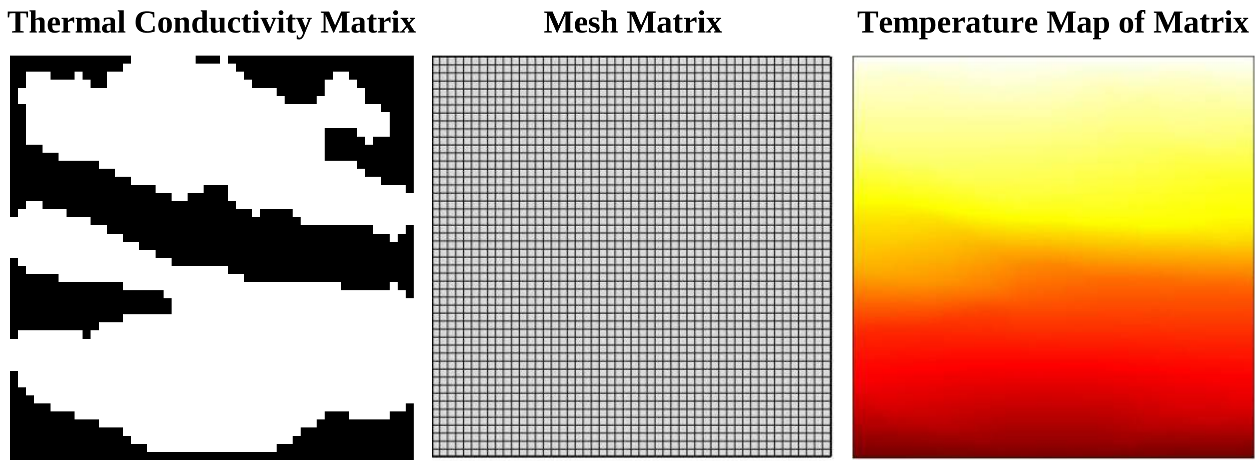

Figure 4. Image Model - Laboratory formed THF hydrate + Kaolinite mixture

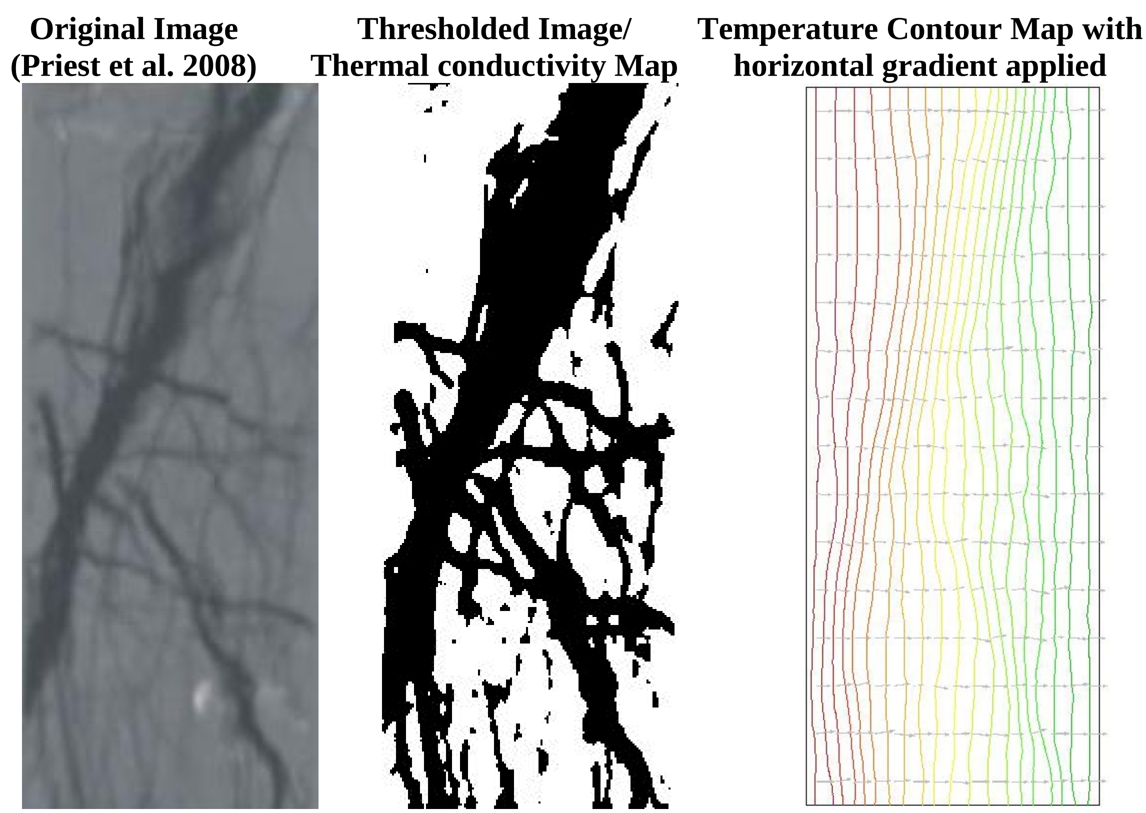

Figure 5. Image Model – In-situ natural gas hydrate + marine sediment

The thermal properties used in this case are of CH_4 hydrate and saturated marine clay from Table 1:

- Volume fraction of hydrate in medium – 36.76%
- Effective thermal conductivity in the vertical direction when medium is subjected to a 50K vertical thermal gradient – 0.806W m^{-1} K^{-1}
- Effective thermal conductivity in the horizontal direction when medium is subjected to a 50K horizontal thermal gradient – 0.869W m^{-1} K^{-1}
- Volume fraction of hydrate – 43.55%
- Effective thermal gradient in vertical direction – 0.830W m^{-1} K^{-1}
- Effective thermal gradient in horizontal direction – 0.780 W m^{-1} K^{-1}

This preliminary study provides great insight into the variability of the effective properties due to the topology of hydrate lenses.

CO_2 Hydrate Formation

Tests were conducted to form CO_2 hydrate in diatomaceous earth. Water was injected into the system outside of hydrate stability field in test 1 (Figures 6 and 7) and inside the stability field in test 2 (Figures 8, 9 and 10). In both tests, oven dried specimen with built-in thermocouples were placed into a high pressure chamber. Several vacuum-CO_2 flooding cycles were conducted to increase CO_2 saturation and remove all N_2. Droplets of water were gradually added to the specimen.

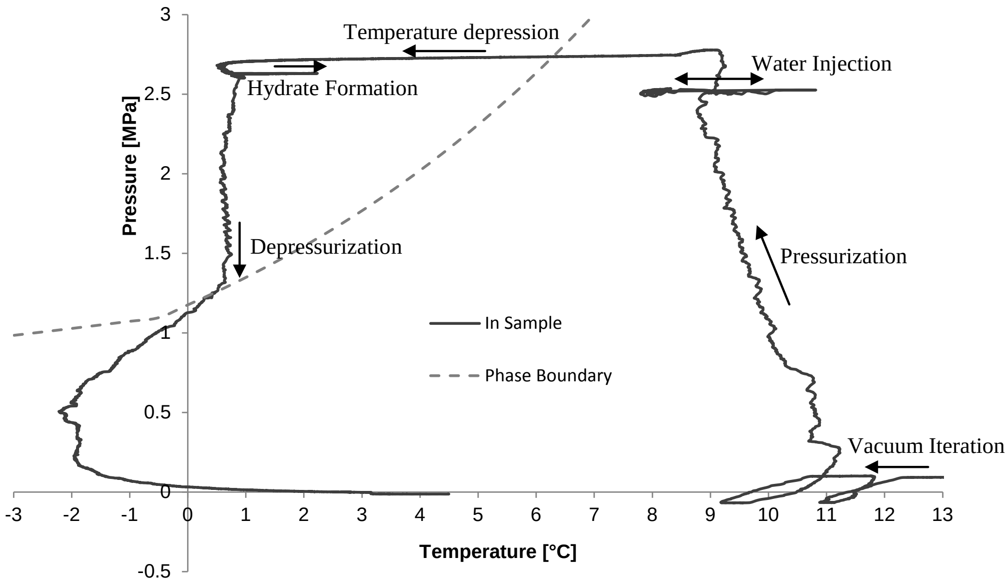

Figure 6. Temperature-Pressure path for test 1

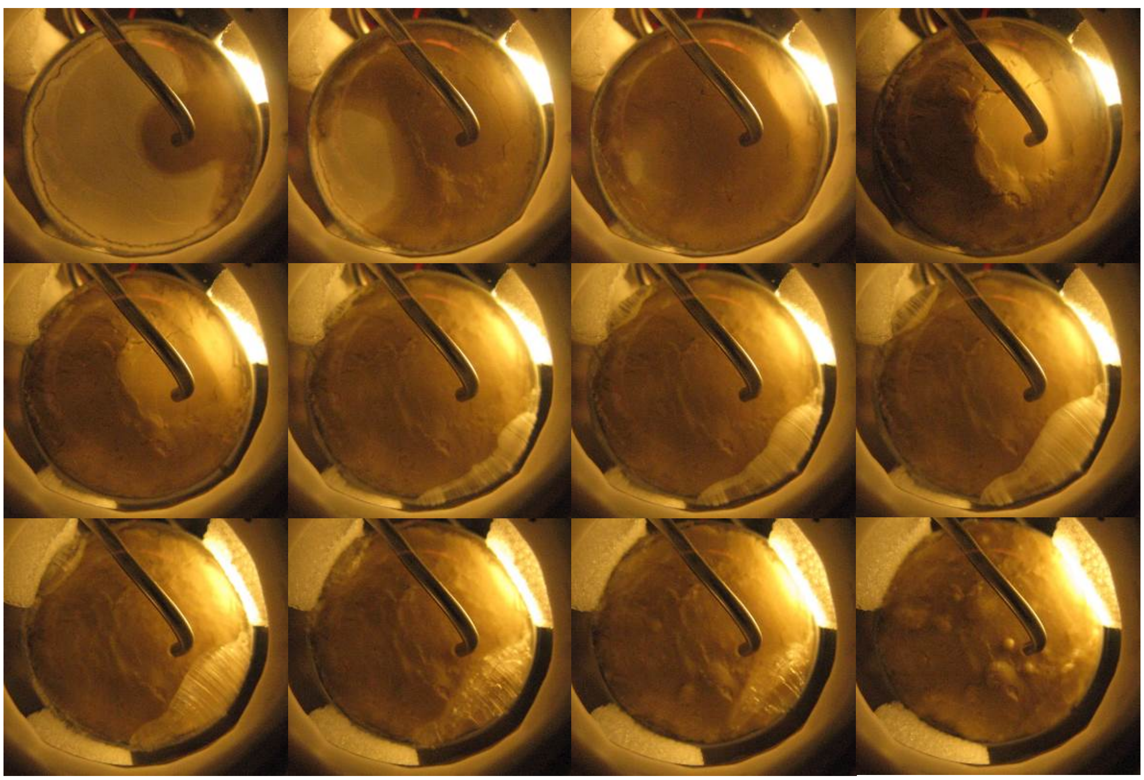

Figure 7. Pictures taken during the wetting process inside the stability field (the first row corresponds to the 'Water Injection', the second row 'Hydrate Formation', and the third 'Depressurization')

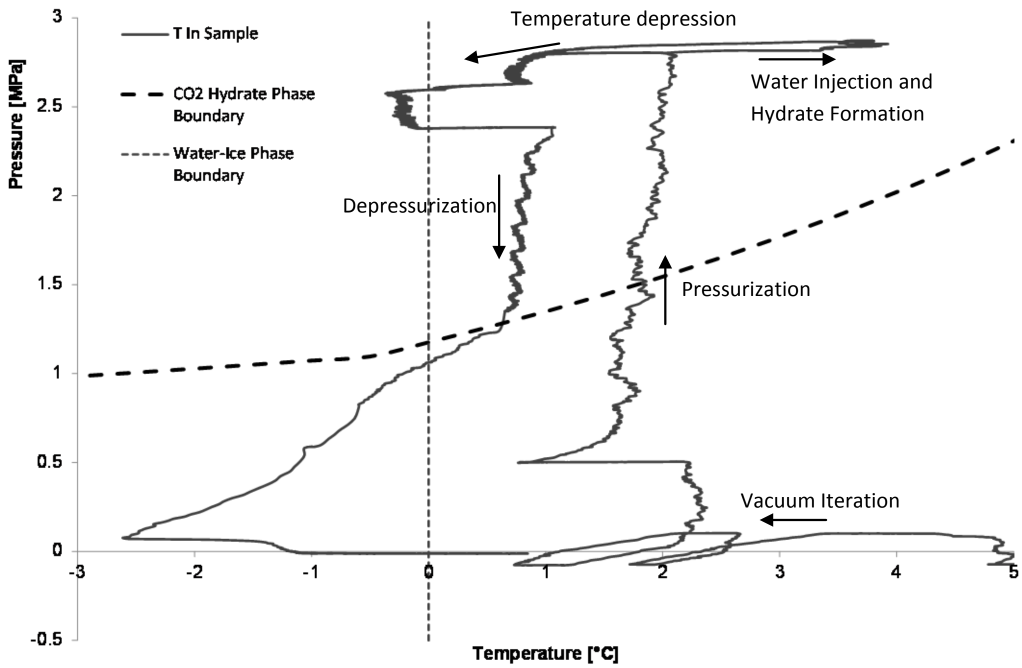

Figure 8. Temperature-Pressure path for test 2

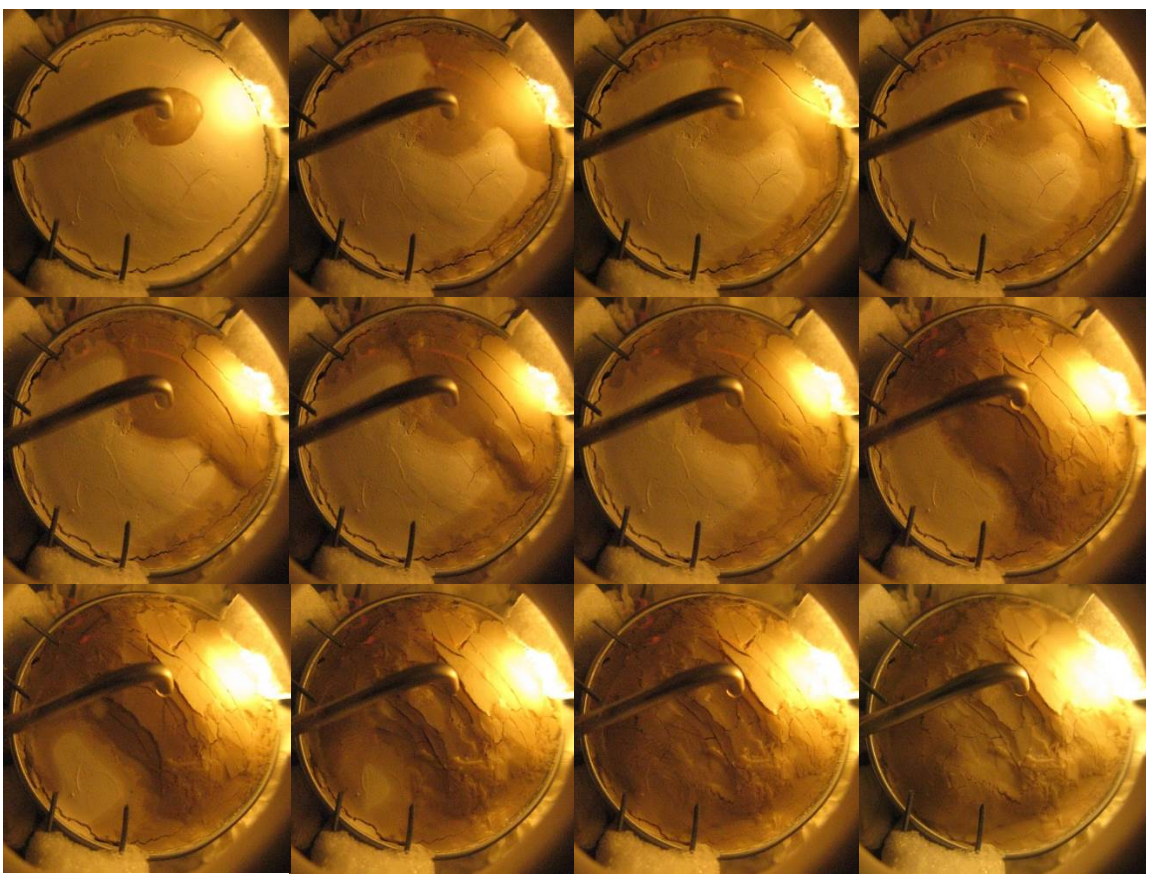

Figure 9. CO_2 Hydrate formation with water droplet added to the specimen (This corresponds to "Water Injection and Hydrate Formation" in the P-T path)

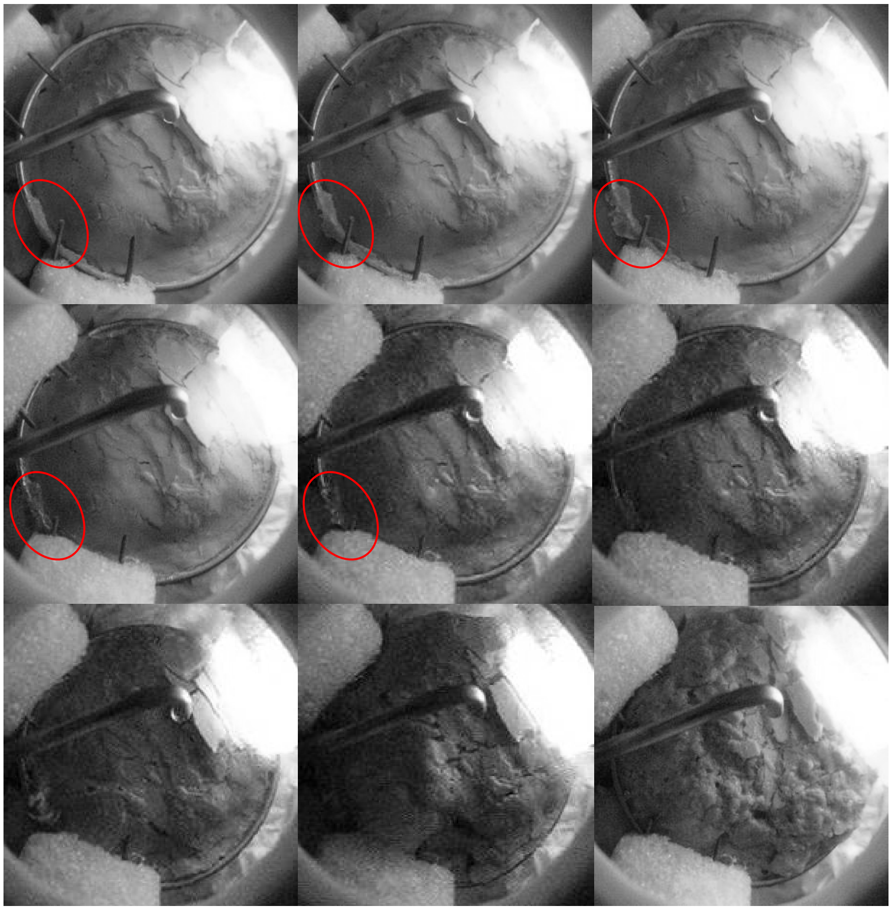

Figure 10. Growth (notice the crystal on the edge of the container) and dissociation of CO_2 hydrate (Images captured from low resolution video)

Observations:

- Cracks formed during water injection contract and vanish during hydrate formation.
- Hydrate continues growing even after PT equilibrium. Slow ice crystal formation on edges and cracks draws water from the sediment.
- Dissociation causes massive sediment disruption in this unconfined test. Yet, some of the initial sediment structure is preserved after dissociation, which indicates segregated hydrate formation.

THF Hydrate Formation in Clay

THF hydrate was formed in three distinct fine-grained geomaterials: diatoms, kaolinite, and silica flour. The samples were formed by first creating a THF-H_2O solution above stoichiometric ratio 1THF:13H_2O to ensure that no ice forms in the system. After thoroughly mixing the selected geomaterials with the fluid at a liquid content similar to that of each of the materials' liquid limits, the specimens were placed in the aluminum chamber. Two thermocouples were positioned in the specimens, one directly in the center and the other ~0.5 cm below the surface and ~0.2cm from the aluminum wall, shown in figure 11. Each of the specimens was then CT-imaged to assess the initial sediment structure and the presence of air voids. Then, specimen where subjected to temperature controlled conditions to bring the mixture inside the stability field. Thermal spikes showed hydrate formation (Figure 12). Finally, specimens were scanned again to visualize the topology of the hydrate.

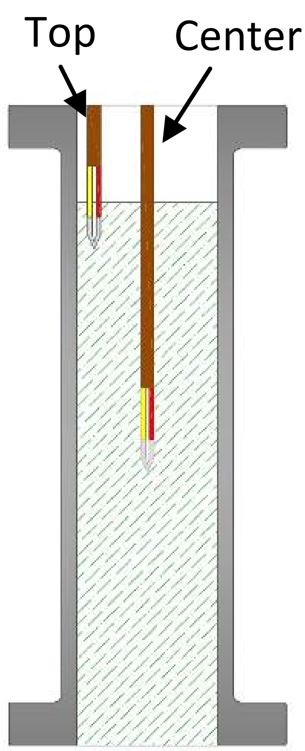

Figure 11. Schematic of thermocouples in X-ray invisible high pressure chamber

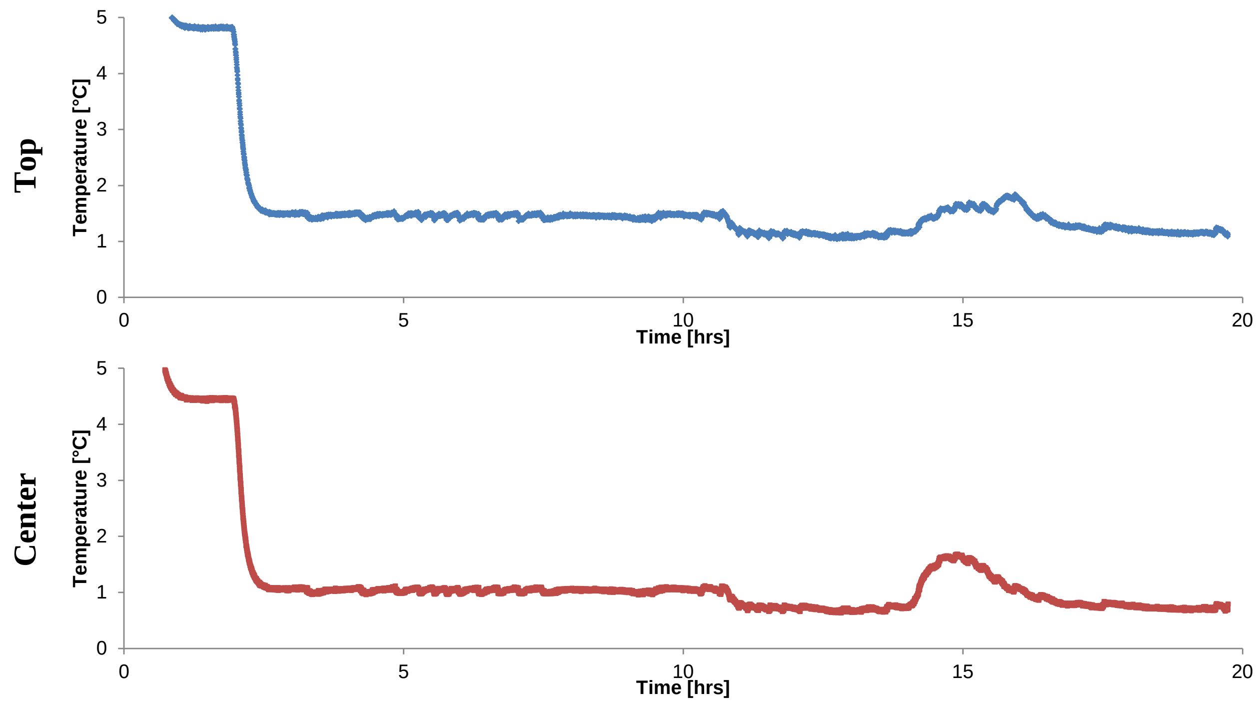

Figure 12. Thermal signatures (Kaolinite specimen)

Slices of the 3D tomographic image gathered after hydrate formation are shown next. In general, thicker but fewer lenses formed in diatoms, while thinner and more lenses formed in kaolinite. A structure of fine lenses occurred on the outer diameter of the kaolinite specimen. No lenses were detected in the silica flour, though hydrate did noticeably form coating air voids created during sample preparation. These results are in agreement with previous observations made by this group on the topology of hydrate formation in sediments.

Diatom + THF Hydrate

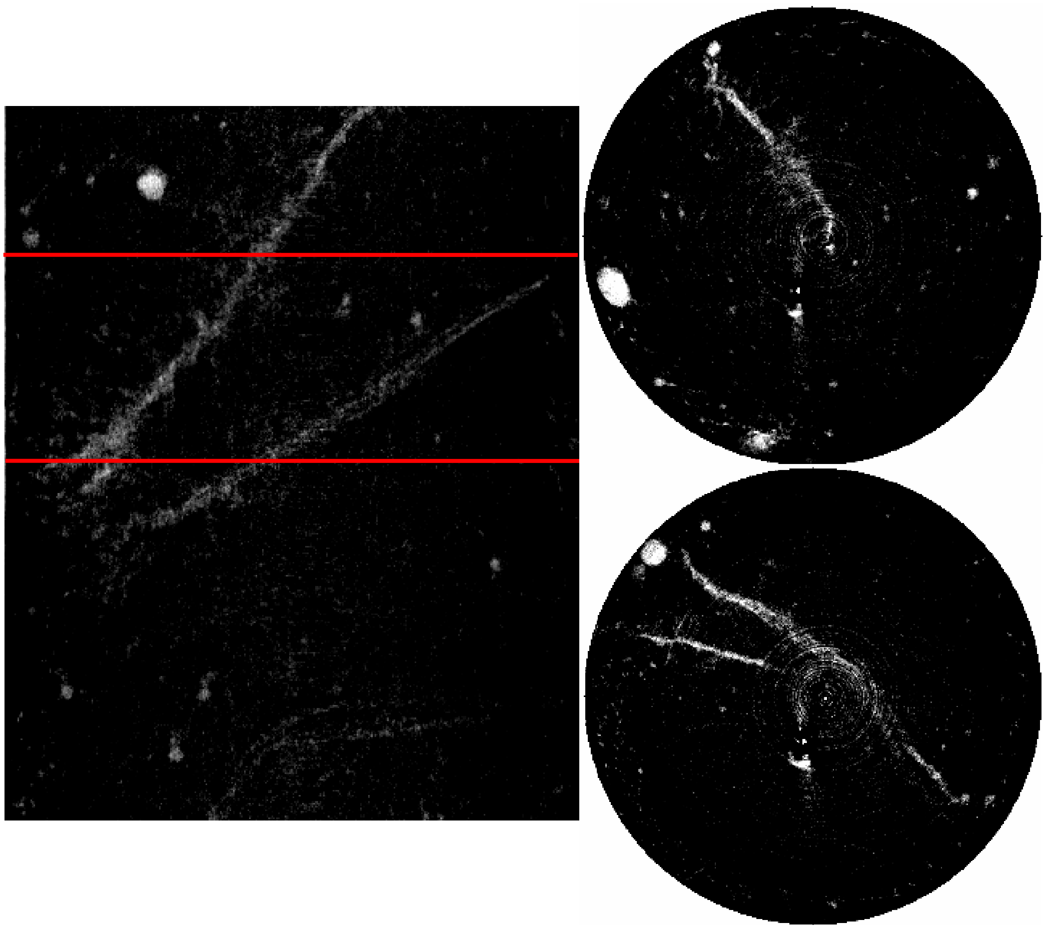

Kaolinite + THF Hydrate

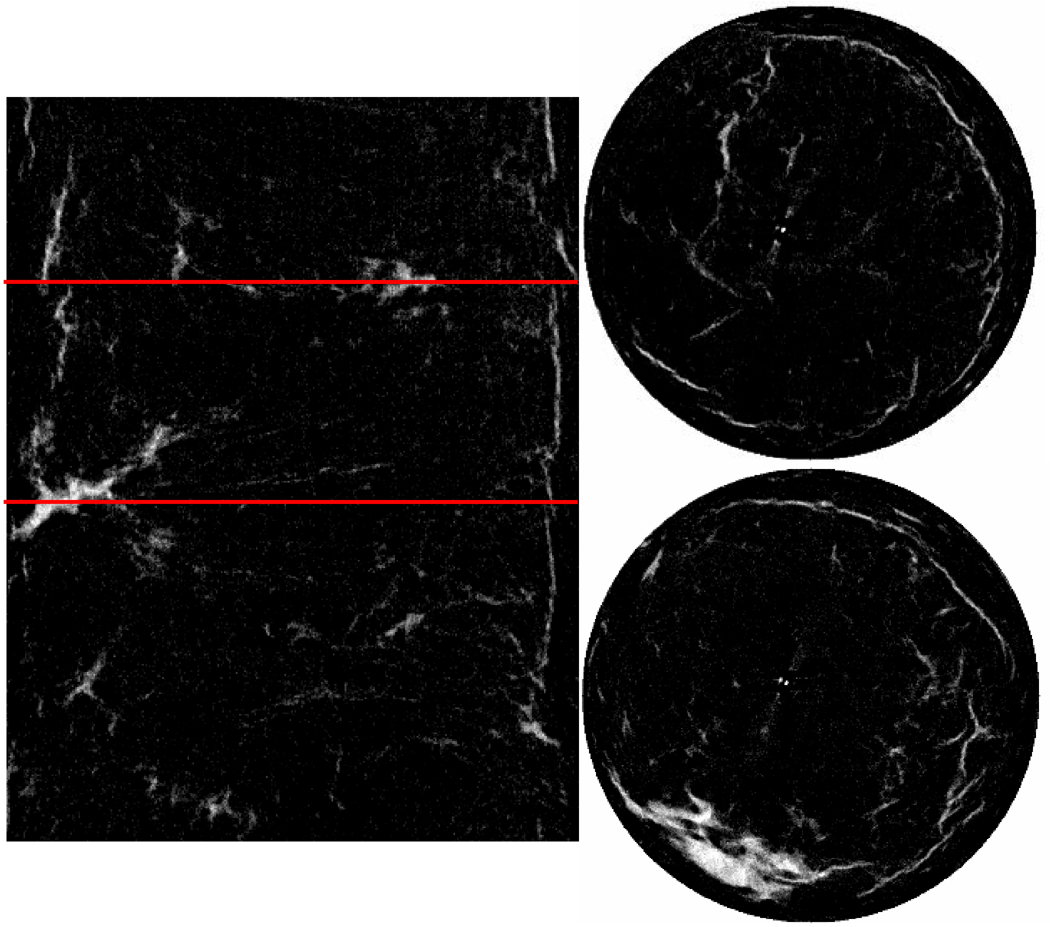

Silica Flour + THF Hydrate

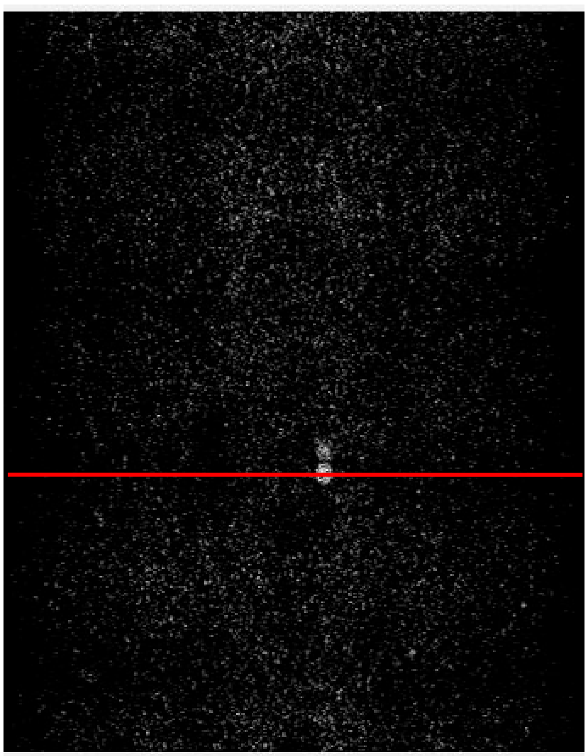

MILESTONE LOG

Milestone	Planed completion date	Actual completion date	Verification method	Comments
Literature review	5/2013	5/2013	Report	Completed first phase. Will continue throughout the project
Preliminary laboratory protocol	8/2013	8/2013	Report (with preliminary validation data)	this and previous reports
Cells for Micro-CT	8/2013	8/2013	Report (with first images)	this and previous reports
Compilation of CT images: segregated hydrate in clayey sediments	8/2014	In progress	Report (with images)	
Preliminary experimental studies on gas production	12/2014		Report (with images)	
Analytical/numerical study of 2-media physical properties	5/2015	In progress	Report (with analytical and numerical data)	
Experimental studies on gas production	12/2015		Report (with data)	
Early numerical results related to gas production	5/2016	In progress	Report	
Comprehensive results (includes Implications)	9/2016		Comprehensive Report	

PRODUCTS

- **Publications:**

  Viggiani, G., Andò, E., Takano, D, and Santamarina, J.C., X-ray Tomography: A Valuable Experimental Tool for Revealing Processes in Soils, ASCE Journal of Geotechnical and Geoenvironmental Engineering. Submitted.

- **Presentations:**
- **Website:** Publications and key presentations are included in http://pmrl.ce.gatech.edu/ (for academic purposes only)
- **Technologies or techniques:** X-ray tomographer and pressure vessel
- **Inventions, patent applications, and/or licenses:** None at this point.
- **Other products:** None at this point.

PARTICIPANTS & OTHER COLLABORATING ORGANIZATIONS

Research Team: The current team is shown next. We anticipate including external collaborators as the project advances

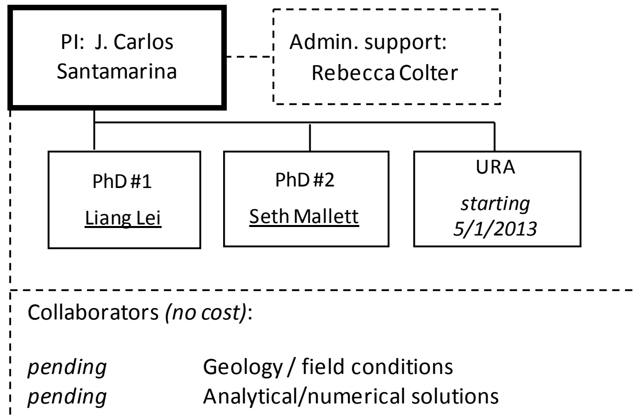

IMPACT

While it is still too early to assess impact, we can already highlight preliminary success of exploring hydrate lenses morphology in real systems, and analogue studies using a high resolution tomographer.

CHANGES/PROBLEMS:

None at this point.

SPECIAL REPORTING REQUIREMENTS:

We are progressing towards all goals for this project.

BUDGETARY INFORMATION:

As of the end of this research period, expenditures are summarized in the following table.

Note: in our academic cycle, higher expenditures typically take place during the summer quarter.

Baseline Reporting Quarter	Budget Period 1									
	Q1		Q2		Q3		Q4		Q1	
	10/1/12 - 12/31/12		1/1/13 - 3/31/13		4/1/13 - 6/30/13		7/1/13 - 9/30/13		10/1/13 - 12/31/13	
	Q1	Cumulative Total	Q2	Cumulative Total	Q3	Cumulative Total	Q4	Cumulative Total	Q1	Cumulative Total
Baseline Cost Plan										
Federal Share	39,212	39,212	39,212	78,424	39,212	117,636	39,212	156,848	39,212	196,060
Non-Federal Share	11,423	11,423	11,423	22,847	11,423	34,270	11,423	45,694	11,423	57,117
Total Planned	50,635	50,635	50,635	101,271	50,635	151,906	50,635	202,542	50,635	253,177
Actual Incurred Cost										
Federal Share	0	0	16,173	16,173	20,191	36,364	66,556	102,920	35,434	138,355
Non-Federal Share	0	0	52,426	52,426	13,106	65,532	0	65,532	0	65,532
Total Incurred Costs			68,600	68,600	33,297	101,897	66,556	168,453	35,434	203,887
Variance										
Federal Share	-39,212	-39,212	-23,039	-62,251	-19,021	-81,272	27,344	-53,928	-3,778	-57,706
Non-Federal Share	-11,423	-11,423	41,003	29,580	1,682	31,262	-11,423	19,839	-11,423	8,415
Total Variance	-50,635	-50,635	17,964	-32,671	-17,339	-50,010	15,921	-34,089	-15,201	-49,291

National Energy Technology Laboratory

626 Cochrans Mill Road
P.O. Box 10940
Pittsburgh, PA 15236-0940

3610 Collins Ferry Road
P.O. Box 880
Morgantown, WV 26507-0880

13131 Dairy Ashford Road, Suite 225
Sugar Land, TX 77478

1450 Queen Avenue SW
Albany, OR 97321-2198

Arctic Energy Office
420 L Street, Suite 305
Anchorage, AK 99501

Visit the NETL website at:
www.netl.doe.gov

Customer Service Line:
1-800-553-7681